Astron. Astrophys. 344, 499–504 (1999)

ASTRONOMY AND ASTROPHYSICS

Extended mid-infrared emission around the outflow source and the compact H II region in AFGL 4029⋆

A. Zavagno[1], **P.O. Lagage**[2], **and S. Cabrit**[3]

[1] Observatoire de Marseille, 2 Place Le Verrier, F-13248 Marseille Cedex 4, France
[2] DSM/DAPNIA Service d'Astrophysique, CEA/Saclay, F-91191 Gif-sur-Yvette cedex, France
[3] Observatoire de Paris, DEMIRM, URA 336 du CNRS, 61 Avenue de l'Observatoire, F-75014 Paris, France

Received 7 September 1998 / Accepted 21 January 1999

Abstract. We present the first sub-arsecond 8–13 μm images of the young stellar cluster AFGL 4029, obtained using the camera CAMIRAS mounted at the Canada-France-Hawaii Telescope.

The two dominant components of the cluster, a highly obscured young stellar object (YSO) and a compact H II region excited by a B1 star, are both spatially resolved and show the 11.3 μm band in emission. The dust composition and excitation in the AFGL 4029 H II region appear similar to those in other compact H II regions of moderate excitation observed by ISO-SWS. In addition, we observe that the 11.3 μm feature/continuum ratio decreases toward the main exciting star on scales $\leq$ 8800 AU. The large extent of the mid-infrared emission from the YSO is so far a unique example among deeply embedded objects. It suggests that there is no simple trend relating the mid-IR size and the evolutionary status in young stars. The emission arises in optically thin circumstellar dust, possibly in a cavity carved by the bipolar outflow.

An optical and near-infrared reflection nebulosity present 5″ away from the YSO is also detected in the mid infrared. It is particularly bright in the 11.3 μm feature, with a feature/continuum ratio $\sim$ 4 comparable to that seen in prototypical reflection nebulae. Finally, mid-IR emission associated with an optical jet knot in the same zone suggests that shocks, by creating small particles, might explain the high surface brightness in this region.

Key words: stars: imaging – stars: individual: AFGL 4029 – stars: pre-main sequence – infrared: ISM: continuum – infrared: ISM: lines and bands – infrared: stars

1. Introduction

Various models have been proposed to reproduce the observed spectral energy distribution of pre-main-sequence stars of intermediate mass, i.e. Herbig Ae/Be stars. An important point is whether to interprete the mid-infrared (mid-IR) excess as due to emission from an extended envelope or from an accretion disk (Hillenbrand et al. 1992; Natta et al. 1993; Hartmann et al. 1993). Using multi-beam photometry, Prusti et al. (1994) investigated a sample of seven nearby (150 pc) young intermediate mass stars and found that the three most evolved objects have their mid-IR fluxes

dominated by extended emission from transiently heated dust grains over scales of 2400 AU. The measurements can be reproduced by circumstellar shells with steep density gradients ($n \propto r^{-1.5}$) and large inner radii ($\simeq$ 200–400 AU). Spatially resolved imaging in the mid-IR is crucial, however, to clarify the geometry of the emission which turns to be highly complex (see the case of HD 97300, Siebenmorgen et al. 1998). For this purpose, Cabrit et al. (1993) have started a ground-based program of high resolution imaging of luminous bipolar outflow sources using the mid-IR camera CAMIRAS (Lagage et al. 1992). The first results of this program provided evidence for the presence of infrared companions in LkHα 198 (Lagage et al. 1993) and LkHα 234 (Cabrit et al. 1997), and for an extended dust shell around V 921 Sco (Lagage et al. 1995).

We now present sub-arcsecond 8–13 μm imaging observations with CAMIRAS of the luminous bipolar outflow source AFGL 4029 (Snell et al. 1988; Hunter 1997). AFGL 4029 is associated with a young embedded cluster recently studied in the visible and near-IR by Deharveng et al. (1997; see references therein for a complete description of the region). Through a coupled photometric and spectroscopic study, these authors identified two dominant sources in AFGL 4029: the first one (their object 25) is a young stellar object (YSO) of 10^4 $L_\odot$ seen only in scattered light out to 1.6 μm, and suffering about 30 mag of visual extinction. Its spectrum is very similar to that of MWC 1080 (probably an early-type Herbig Be star) with bright and broad hydrogen lines (Hα and the Paschen series) and a bright optically thick infrared triplet of Ca II. An optical jet was discovered nearby by Ray et al. (1990), hence this YSO is the most probable exciting source of the bipolar molecular outflow. The other source (their star 26), located 22″ to the east, is a B1 V star of 5×10^4 $L_\odot$ which ionizes a compact H II region and is surrounded by a cluster of at least 30 B-type stars. These two sources correspond to the two peaks of mid-IR radiation found within the cloud by Beichman (1979), named respectively IRS 1

Send offprint requests to: A. Zavagno (Zavagno@obmara.cnrs-mrs.fr; Lagage@cea.fr; Cabrit@mesioq.obspm.fr)

⋆ Based on observations made at the Canada-France-Hawaii Telescope, operated by the National Research Council of Canada, the Centre National de la Recherche Scientifique, and University of Hawaii

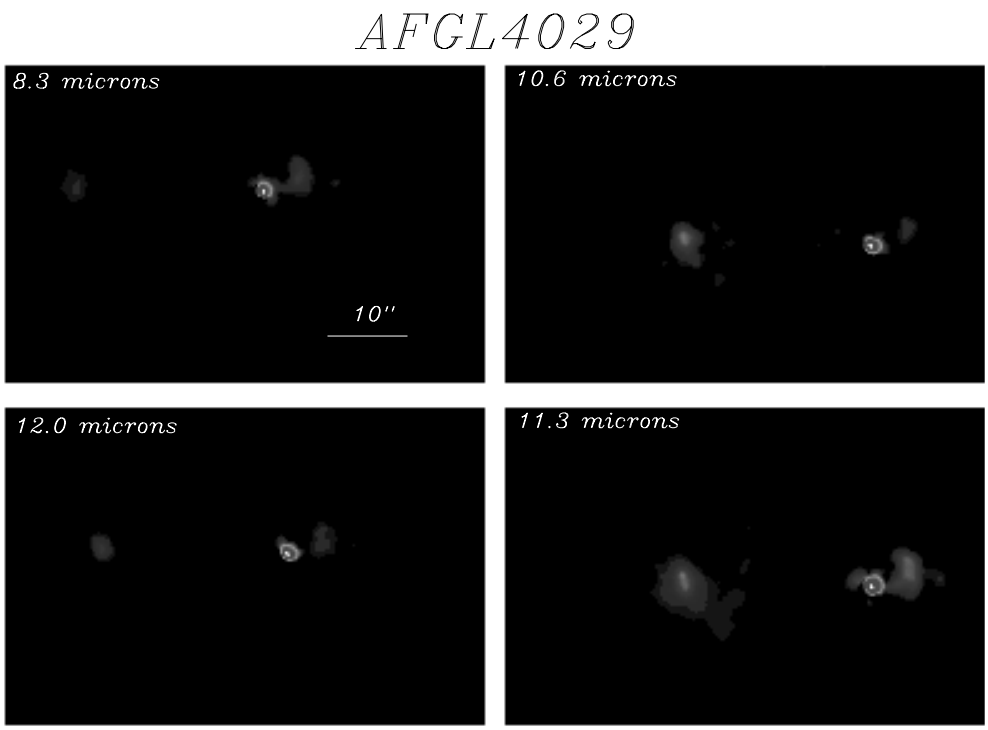

Fig. 1. The AFGL 4029 region observed with CAMIRAS at CFHT in narrow filters at 7.8–8.8 μm (upper left), 10.45–10.85 μm (*upper right*), 11–11.45 μm (*lower right*), 11.77–12.22 μm (*lower left*) after deconvolution by the point spread function. North is up, East is left. The YSO is the bright object to the right and the compact H II region is 22″ to the east. The arc-shaped nebula 5″ north-west of the YSO corresponds to object AFGL 4029 A of Ray et al. (1990). In the 8.3 and 11.23 μm images a fainter knot slightly to the west of the arc-shaped nebula corresponds to knot A of the [S II]-Hα image of the jet (Ray et al. 1990). The pixel size is 0.3″ and the field of view is 57″ ×38″

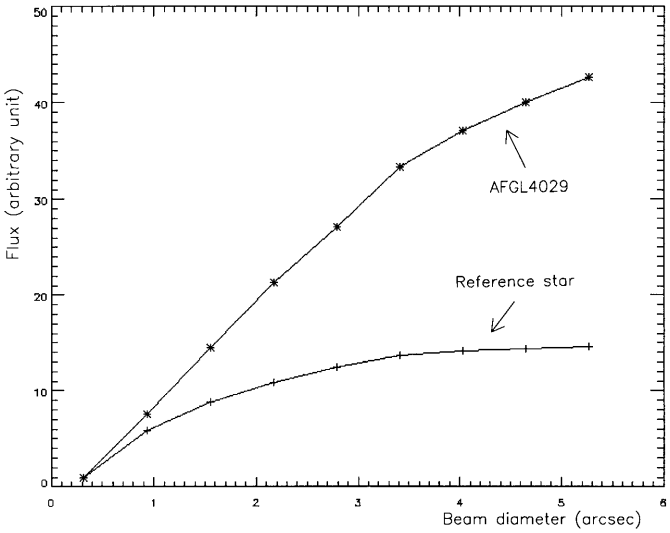

Fig. 2. Aperture photometry (before deconvolution) centered on the YSO (IRS 1), compared to aperture photometry of the reference star γ Aql at 11.23 μm. IRS 1 appears extended all the way down to our resolution limit. Similar results are found in the other three filters

and IRS 2. Beichman found IRS 1 to be unresolved and IRS 2 to be cooler and extended, but could not identify the nature of the emission from lack of adequate spatial and spectral information. Mid-IR arrays and narrow-band filters now allow us to overcome these limitations.

Sect. 2 presents our CAMIRAS results obtained at the Canada-France-Hawaii Telescope (CFHT). Discussion about the origin of the extended mid-IR emission is presented in Sect. 3. Sect. 4 summarizes our conclusions.

2. Imaging and photometry

Observations were made on July 1996 at the CFHT using CAMIRAS (Lagage et al. 1992) equipped with a Si:Ga/DVR detector array of 192×128 pixels (Lucas et al. 1995). The pixel field of view was 0.3″ and the total field of view was 57″ ×38″. The two infrared sources IRS 1 and IRS 2 are both in the field. Four narrow-band filters were used: 7.8–8.8 μm, 10.45–10.85 μm, 11–11.45 μm, 11.77–12.22 μm, in order to look at the continuum emission and to search for the infrared emission bands (hereafter, IEBs) at 8.6 and 11.3 μm characteristic of small carboneous dust grains. Chopping was performed with the wobbling secondary mirror at a frequency of 3 Hz and with a throw of 1′ in declinaison. The nodding frequency was 0.01 Hz. Observations at 10.63 μm and 11.23 μm were done on July 8 during night time. Observations at 8.3 μm and 11.98 μm were done without guiding during day time on July 10, and corrected for tracking errors at the data reduction stage by recentering individual 3 sec images (tracking was good enough that the object did not move on the array during that time).

2.1. Morphology and extension

Fig. 1 shows the CAMIRAS images obtained in the four filters after deconvolution by the point spread function (a reference star) using the algorithm developed by Pantin & Starck (1996). The spatial resolution is 0.9″ (FWHM at 11.23 μm) before deconvolution. The YSO (= IRS 1 of Beichman 1979) is clearly extended at all wavelengths. Even before deconvolution, the integrated flux inside apertures of increasing diameters increases much more than for a point-like reference star, as displayed in Fig. 2 for the 11.23 μm filter. Hence, IRS 1 is dominated by an

Table 1. Mid-IR fluxes for the main components of the AFGL 4029 cluster

Source	$F_{8.3\mu m}$(Jy) (7.8–8.8μm)	$F_{10.63\mu m}$(Jy) (10.45–10.85μm)	$F_{11.23\mu m}$(Jy) (11–11.45μm)	$F_{11.98\mu m}$(Jy) (11.77–12.22μm)
IRS 1 central (1.5″ beam)	3.84 (0.03)	3.44 (0.04)	5.59 (0.03)	5.31 (0.07)
IRS 1 envelope (3.4″ beam)	1.37 (0.04)	1.08 (0.05)	2.67 (0.04)	1.49 (0.08)
Arc-shaped nebulosity (2.4″ ×3.9″)	1.12 (0.05)	0.50 (0.05)	2.82 (0.04)	0.86 (0.09)
H II region (8.1″ beam)	2.00 (0.12)	2.1 (0.11)	4.4 (0.09)	2.5 (0.19)
total (57″ ×38″)	17.4 (0.7)	12.0 (0.7)	33.0 (0.5)	13 (1)

Note: the rms photon noise is given in parentheses. Photometric uncertainty is 8%.

extended component all the way down to our resolution limit. A similar result is found in the other three filters.

Five arcseconds north-west of IRS 1, we observe an arc-shaped emission region that agrees very well with the nebula seen at H and K' by Deharveng et al. (1997). This mid-IR arc corresponds also well to the feature named AFGL 4029 A in the [SII]-Hα image of Ray et al. (1990). We thus confirm Ray et al. (1990) suggestion that AFGL 4029 A is probably purely a reflection knot, while their compact feature AFGL 4029 B is closer to the true location of the YSO (which is only directly seen at wavelengths longer than 2.2 μm; Deharveng et al. 1997).

A few arcseconds more to the west, we see a faint emission knot (most prominent in the 11.3 μm filter) that coincides with knot A of the [S II]-Hα image of the jet (Ray et al. 1990).

IRS 2 is detected 22″ east of IRS 1. The associated emission is centered on the main exciting star of the compact H II region (the B1 V star No. 26 in Deharveng et al. 1997) and is very extended, with a core-halo morphology. The brightest part delineates an ellipse of diameter of about 4″ that corresponds to the associated free-free radio emission (Kurtz et al. 1994; Fig. 5 of Deharveng et al. 1997) and to the location of the brightest members of the cluster. Fainter diffuse emission extends out to larger distance (12″ $\simeq$ 0.1 pc from the center of the H II region), especially to the south-west. This extension follows well the diffuse emission seen around the H II region in the K'-band (Fig. 5 of Deharveng et al. 1997).

2.2. Photometry and spectral energy distributions

Photometric calibration was done using the reference stars γ Aql (HD 186791, with N-magnitude -0.78; Tokunaga 1984) and β And (HD 6860, see Cohen et al. 1995 for the flux in various filters), observed on July 8. Air mass correction had to be taken into account in the case of β And. Flat field correction was performed using high signal-to-noise sky images at 1 and 2 air masses.

The photometric results are given in Table 1. In order to search for spectral gradients between the inner and outer envelope of IRS 1, its flux was arbitrarily split into two parts: the 'central part' of IRS 1 was estimated from the flux measured in a 1.5″ undeconvolved beam. The contribution of the central part beyond 1.5″ was then removed using the PSF. The 'outer envelope' of IRS 1 corresponds to the remaining circumstellar emission as measured in a 3.4″ beam (this rather small beam size

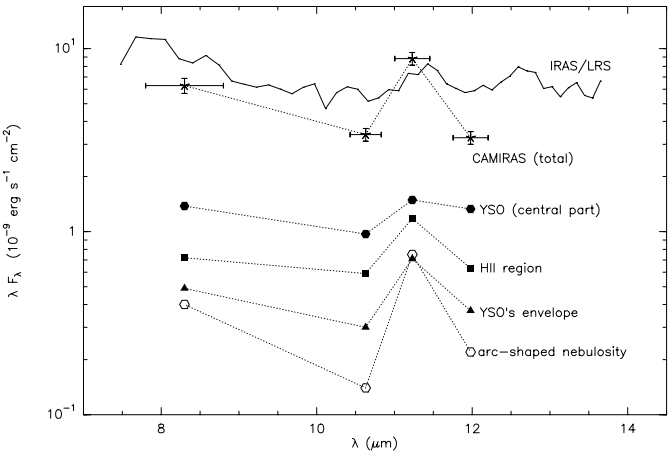

Fig. 3. Spectral energy distributions of the dominant mid-IR sources in the AFGL 4029 cluster. The total flux integrated over the whole CAMIRAS field (before deconvolution) shows the filters width and the typical photometric uncertainty

was chosen to avoid confusion with the arc-shaped nebulosity). Flux from the arc-shaped nebulosity itself was measured in a rectangular beam of 2.4″ ×3.9″ centered on the peak emission of the nebulosity at ($\Delta\alpha$,$\Delta\delta$) = (-4.6″, +1.8″). The photometric uncertainty is typically 8%.

Fig. 3 presents the spectral energy distributions between 7.8 and 12 μm of the central part of IRS 1, its outer envelope, the associated arc-shaped nebulosity, and IRS 2. The IRAS Low Resolution Spectrum (IRAS, 1988) of the infrared source IRAS 02575+6017 associated with the AFGL 4029 cluster is also shown in Fig. 3 for comparison. There is good agreement between the IRAS/LRS and the total flux integrated over the whole CAMIRAS field. The IRAS/LRS spectrum suggests that the 8.6 and 11.3 μm emission bands are present toward AFGL 4029. The CFHT data show that the 11.3 μm emission band is indeed present in the 'envelope' of IRS 1 and in the arc-shaped nebulosity, as well as in IRS 2. If we estimate the continuum level by interpolating between the 10.6 μm and 12.0 μm fluxes, the band+continuum over continuum ratio, defined as $F_{11.3+cont}/F_{cont}$, ranges from 2.0 (in the YSO envelope and the H II region) to 4 (in the arc-shaped nebula). The situation is less clear-cut for the central part of IRS 1: the band+continuum/continuum ratio is low (at most 1.3) and silicate absorption at 9.7 μm, expected in highly embedded objects,

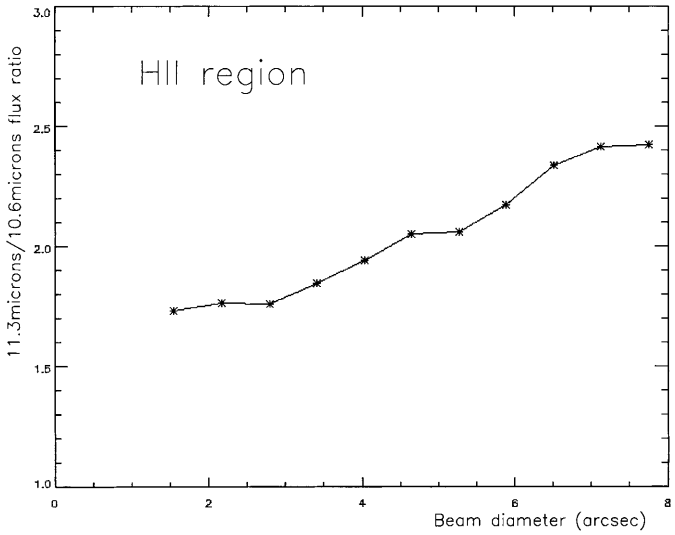

Fig. 4. Variation of the band+continuum/continuum ratio (11.23/10.63) as a function of distance, in arcsec, from the center of IRS 2 (the compact H II region)

could strongly affect the continuum shape. Note that our measured band+continuum to continuum ratio is a lower limit to the true peak ratio as the width of the 11.23 μm filter, 0.5 μm, is slightly larger than the intrinsic band width observed in ISO-SWS spectra (e.g. Verstraete et al. 1996). Where the 11.3 μm emission feature is present, flux at 8.3 μm is higher than the continuum level at 10.6 μm and 12.0 μm. The 8.3 μm filter probably contains a contribution from the 8.6 μm and part of the 7.7 μm IEBs (which are usually simultaneously present with the 11.3 μm).

3. Discussion

The infrared emission bands (IEBs) at 3.3, 6.2, 7.7, 8.6 and 11.3 μm have been spectroscopically detected in a number of Herbig Ae/Be stars either by the IRAS-LRS (Zavagno et al. 1992) or by ground-based facilities (Brooke et al. 1993 and references therein; Wooden 1994). Various candidates have been proposed for the band carriers: polycyclic aromatic hydrocarbon molecules and ions (PAHs; Léger & Puget 1984; Allamandola et al. 1985), hydrogenated amorphous carbon (HAC; Borghesi et al. 1987), quenched carbonaceous components (QCC; Sakata et al. 1984) and coal grains (Papoular et al. 1989; Papoular et al. 1996).

Our spectral resolution is much poorer than that available with ISO-SWS (de Graauw et al. 1996) or ISOCAM-CVF (Cesarsky C. et al. 1996), and thus does not allow us to distinguish between these various possibilities. However, our sub-arcsecond spatial resolution allows us to precisely locate the mid-IR emission and to trace feature/continuum changes down to smaller scales than possible with ISO. In the following, we compare our data with results from ground-based and ISO spectroscopy of similar sources to discuss the possible nature of the IEBs' carriers, the spectral type of the exciting stars and the evolutionary status of the YSO.

3.1. IRS 2: warm dust in the compact H II region

We have compared the mid-IR spectral energy distribution obtained for IRS 2 (Fig. 3) with the shape of ISO-SWS spectra toward six compact H II regions (Roelfsema et al. 1996). Despite the differing beam sizes (8.1″ here, about 20″ for the ISO-SWS) we find that the observed narrow-band filter ratios are perfectly consistent with the typical spectrum of H II regions of moderate excitation ($L_{bol} \leq 5 \times 10^4$ L$_\odot$). In regions of higher UV fields, a strong rising continuum is present, which strongly reduces the feature/continuum contrast (see also M 17; Vestraete et al. 1996). We may in fact be witnessing such a contrast effect at small scales within IRS 2 itself: Fig. 4 presents the variation of the band+continuum over continuum ratio $R = F_{11.23}/F_{10.63}$ in IRS 2 as a function of distance from the center. The ratio decreases from 2.5 to 1.5 as we get closer to the central exciting star. This suggests a strong contribution from the thermal continuum of warmer grains in the ionized zone as observed in galactic H II regions (Zavagno & Ducci 1999, Tran et al. 1999). This could also be due to PAH dehydrogenation near the star that would decrease the 11.3 μm contribution.

Finally, we have found a halo of 11.3 μm emission extending well beyond the ionized region out to 12″ = 0.1 pc from the central star, i.e. into the surrounding molecular cloud. The situation is reminiscent of M 17, where Cesarsky D. et al. (1996) and Verstraete et al. (1996) have found strong infrared emission bands extending well beyond the photodissociation front. Our data show that this phenomenon also occurs around an H II region of lower excitation.

3.2. IRS 1: a young embedded early-type star

The characteristics of IEBs in Herbig Ae/Be stars can be a good indicator of stellar spectral type: they are more frequently detected around stars earlier than B6 (Wooden 1994) and the feature flux increases roughly in proportion to the stellar UV flux (Brooke et al. 1993; see also Zavagno et al. 1992). In the 3.3 μm band, the emission *size* also tends to increase with stellar temperature, an effect attributed to PAH dehydrogenation (which removes the 3.3 μm C-H feature) close to the star (Brooke et al. 1993). If this interpretation is correct, we would expect a similar trend in the 11.3 μm band, since it is also due to a C-H bond.

Little data is available so far about spatial extension in the 11.3 μm feature. Prusti et al. (1994) performed N_1, N_2, and N-band photometry of a sample of Herbig Ae/Be stars at 150 pc, with two beams of diameters 5.4″ = 800 AU and 16″ = 2400 AU. They found indication of an evolutionary trend, in the sense that stars with the largest IR excesses are dominated by a compact component in N_1 (90% of the flux inside 1200 AU comes from within $R < 400$ AU) while those with little circumstellar matter and no Hα emission activity are dominated by extended halos of emission, presumably from IEBs (only 20% of the N_1 flux within $R < 400$ AU). However, they could not exclude substantial halos around stars with a bright compact component.

Our image of IRS 1 provides, to our knowledge, the first clear example of an embedded YSO with large amounts of cir-

cumstellar matter that does possess an extended halo of 11.3 μm emission on the scale probed by Prusti et al. (1994): at the distance of AFGL 4029 (2.2 kpc, see Deharveng et al. 1997), beam diameters of 800 AU and 2400 AU subtend 0.37″ and 1.1″ respectively. Fig. 2 shows that in this object, at most 75% of the flux inside R=1200 AU comes from within $R < 400$ AU; this value is an upper limit because of smearing by the PSF. A similar fraction of 68% was found in the Hα active Herbig Be star HD 97048 by Prusti et al. (1994), but that star is optically visible and is therefore probably at a later evolutionary stage than IRS 1. If we adopt a typical outer radius of 5″≅ 11000 AU for the 11.3 μm emission band in IRS 1, Fig. 4 of Brooke et al. (1993) would then suggest an effective temperature of about 20000 K, i.e. a spectral type of B3.

The large extension of mid-IR emission in IRS 1 has important implications for its circumstellar structure: Models of dust emission in circumstellar envelopes (using the model of Siebenmorgen & Krügel 1992) show that such a continued flux increase at 10 μm over large scales is only encountered in optically thin dust envelopes; else emission is dominated by the innermost radius, where most of the UV flux is absorbed (Siebenmorgen, private communication). A reasonable fit to Fig. 2 is obtained for an inner radius of $\leq 3 \times 10^{16}$ cm and a rather flat density distribution, assuming that the relative abundance of PAHs and graphite grains with respect to hydrogen is constant throughout the envelope. If the carriers of the 11.3 μm C-H band were significantly depleted in the inner regions (e.g. due to PAH dehydrogenation), the true gas density would have to fall out more steeply to reproduce the data. A detailed model taking into account these effects is beyond the scope of this paper.

The fact that the envelope is optically thin is surprising in view of the very large visual extinction of 30 mag suffered by IRS 1 and of the large amount of circumstellar material indicated by submillimetre measurements (Hunter 1997). A possible explanation is that the extinction comes from a flattened and compact structure, i.e. a circumstellar disk, while the optically thin dust is located in a cavity carved by the powerful outflow from the YSO. Evidence for an anisotropic distribution of material in the close vicinity of IRS 1 is independently provided by 2 μm speckle imaging which shows a halo shifted from the stellar position (Leinert et al. 1994). Part of the extinction may also arise in swept-up dense ambient material on the line of sight between the cavity and the observer.

3.3. The arc-shaped nebulosity and the jet knot A

No internal source of heating was detected in the arc-shaped nebulosity down to a sensitivity limit of 0.05 Jy. This non-detection is consistent with the fact that the near-IR colours of the arc-shaped extension are equivalent to those of visual reflection nebulae (see Fig. 4 in Deharveng et al. 1997 and also Hartmann et al. 1993). The YSO IRS 1, located 5″ away, seems the most probable illuminating source of this nebula. An implication is that very small grains are probably present, to explain the near-IR emission longward of 1 μm (Sellgren 1984). Our mid-IR observations set further constraints on the possible nature of these small grains.

In Fig. 1, the associated arc-shaped extension is clearly seen at the wavelengths of the two emission features (8.6 and 11.3 μm filters), but it is much fainter in the continuum filters. The feature to continuum ratio reaches here its maximum value of 4. Coal grains heated by the 10^4 $L_\odot$ YSO could achieve a temperature $\simeq$ 300 K (Guillois et al. 1994), sufficient to emit in the mid-IR at the distance of the nebula. However, the high value $\simeq$4 of the 11.3 μm feature over continuum ratio is not explained, as the observed band over continuum ratio for coal grains in the laboratory is always smaller than 3 (Papoular, private communication). 'Non-classical' excitation mechanisms for coal grains are being studied (Guillois et al. 1998), but it is not yet clear whether they will explain such a high observed band over continuum ratio.

The mid-IR spectral shape and filter ratios in the arc-like nebula in Fig. 3 are extremely similar to those observed by ISOCAM-CVF in the prototypical reflection nebula NGC 7023 (Cesarsky D. et al. 1996b). There, emission peaks in a filament 28″ away from the young Herbig B3Ve star HD 200775. Given its distance of 440 pc, it corresponds to 12300 AU, close to the 11000 AU that separate here AFGL 4029-IRS 1 and its nebula. It is thus reasonable to propose that the same kind of grains are responsible for the mid-IR emission in both regions. One important difference, however, is that the 11.3 μm surface brightness is roughly 10 times higher in the AFGL 4029 nebula: the peak flux at 11.3 μm is 2.8 Jy inside 2.4″ × 3.9″, while in NGC 7023 it is only 1 Jy inside a 6″ pixel. Part of the difference could stem from our higher spatial resolution. Another, more speculative, explanation for such a high mid-IR brightness would be the presence of wind-driven shocks in the nebula around AFGL 4029: shocks, by destroying big grains, can enhance locally the abundance of smaller particles (Jones et al. 1996), and therefore increase the mid-IR emission. The fact that we also detect mid-IR emission toward knot A associated with the optical jet brings support to this interpretation. If confirmed, the creation of small particles in shocks would be very important, as this question remains open (Cox et al. 1998).

4. Conclusions

Sub-arcsecond resolution mid-IR images of AFGL 4029 show that the two main components of this cluster, a YSO and a compact H II region, are seen in the continuum and have the 11.3 μm feature in emission.

(1) Emission from the H II region is centered on the main exciting star. Fainter emission extends beyond the ionized region, out to 12″= 0.1 pc. Comparisons with ISO-SWS results suggest that the dust composition in IRS 2 is similar to that observed in compact H II regions of moderate excitation. This supports the B1 spectral type and luminosity $\sim 5 \times 10^4$ $L_\odot$ inferred for the exciting star (Deharveng et al. 1997). We observe a decrease of the 11.3 μm band to continuum ratio toward the star, suggesting either a strong contribution from thermal continuum in

high UV fields, possibly from coal grains, or the effect of PAH dehydrogenation.

(2) Emission from the YSO (IRS 1) is resolved and comes predominantly from an extended component, as previously believed from the rising shape of its near-IR spectral energy distribution ('Group II' star; Hillenbrand et al. 1992). Surprisingly for an object of this youth, this circumstellar emission is very optically thin; it is probably tracing a wind cavity. The high extinction toward the YSO may then arise in an edge-on dust disk. Like in the H II region, we observe a moderate 11.3 μm feature/continuum ratio ~ 2. If this is due to PAH dehydrogenation, the size of the emission would suggest a B3 spectral type.

(3) The arc-shaped nebulosity already seen at visible and near-IR wavelengths is detected in the mid-IR. The 11.23 μm feature/continuum ratio $\simeq 4$ is similar to that in the prototypical reflection nebula NGC 7023, however the surface brightness is ten times higher. The presence of an optical jet suggests that shocks could play a role in enhancing the abundance of small particles in this region, hence increasing the mid-IR brightness. The detection of 8.3 and 11.23 μm emission toward knot A reinforces the idea of dust particle creation in shocks. If confirmed, this would be the first observational evidence for such a process.

Acknowledgements. We would like to thank R. Jouan and P. Masse for their kind assistance with CAMIRAS observations. We are also grateful to E. Pantin for helping us with his filtering and deconvolution techniques. Finally, we are greatly indebted to R. Papoular for enlightening discussions on dust features, and to R. Siebenmorgen for sharing his expertise on radiative transfer simulations in envelopes containing small dust grains. This research has made used of the Simbad database, operated at CDS, Strasbourg, France.

References

Allamandola L.J., Tielens A.G.G.M., Baker J.R., 1985, ApJ 290, L25
Beichman C.A., 1979, Thesis, University of Hawaii
Borghesi A., Bussoletti E., Colangeli L., 1987, ApJ 314, 422
Brooke T.Y., Tokunaga A.T., Strom S.E., 1993, AJ 106, 656
Cabrit S., Lagage P.O., Pantin E., 1993, In: Mc Lean I. (ed.) Infrared Astronomy with arrays: the next generation. Kluwer, Dordrecht
Cabrit S., Lagage P.O., McCaughrean M., Olofson G., 1997, A&A 321, 523
Cesarsky C., Abergel A., Agnèse P., et al., 1996, A&A 315, L32
Cesarsky D., Lequeux A., Abergel A., et al., 1996, A&A 315, L309
Cesarsky D., Lequeux A., Abergel A., et al., 1996b, A&A 315, L305
Cohen M., Witteborn F.C., Walker R.G., Bregman J.D., Wooden D.H., 1995, AJ 110, 275
Cox P., Boulanger F., Huggins P.J., et al., 1998, ApJ 495, L23
de Graauw Th., Haser L.N., Beintema D.A., et al., 1996, A&A 315, L49
Deharveng L., Zavagno A., Cruz-González I., et al., 1997, A&A 317, 459
Guillois O., Nenner I., Papoular R., Reynaud C., 1994, A&A 285, 1003
Guillois O., Ledoux G., Nenner I., Papoular R., Reynaud C., 1998, Faraday Discuss., 109, in press
Hartmann L., Kenyon S.J., Calvet N., 1993, ApJ 407, 219
Hillenbrand L.A., Strom S.E., Vrba F.J., Keene J., 1992, ApJ 397, 613
Hunter T.R., 1997, Ph.D. Thesis, California Institute of Technology, Passadena, California
IRAS Science Team, 1988, A&AS 65,607
Jones A.P., Tielens A.G.G.M, Hollenbach D.J., 1996, ApJ 469, 740
Kurtz S., Churchwell E., Wood D.O.S., 1994, ApJS 91, 659
Lagage P.O., Jouan R., Masse P., Mestreau P., Tarrius A., 1992, In: Ulrich M.H. (ed.) 42^{nd} ESO Conference; Progress in telescope and instrumentation technologies. ESO, Munich, p. 601
Lagage P.O., Olofsson G., Cabrit S., et al., 1993, ApJ 417, L79
Lagage P.O., Cabrit S., Montmerle T., Olofsson G., 1995, In: Käufl H.U., Siebenmorgen R. (eds.) The Role of Dust in the Formation of stars. ESO Astrophysics Symposia, p. 39
Léger A., Puget J.L., 1984, A&A 137, L5
Leinert C.H., Richichi A., Weitzel N., Haas M., 1994, ASP Conference Series, Vol. 62, 155
Lucas C., Bischoff I., Chammings G., et al., 1995, Development of gallium-doped silicon 128x192 element arrays for 8–14 microns observations. Proceedings SPIE meeting, Volume 2475, p. 50–55
Natta A., Prusti T., Krügel E., 1993, A&A 275, 527
Pantin E., Starck J.L., 1996, A&AS 118, 575
Papoular R., Conard J., Guiliano M., Kister J., Mille G., 1989, A&A 217, 204
Papoular R., Conard J., Guillois O., et al., 1996, A&A 315, 222
Prusti T., Natta A., Palla F., 1994, A&A 292, 593
Ray T.P., Poetzel R., Solf J., Mundt R., 1990, ApJ 357, L45
Roelfsema P.R, Cox P., Tielens A.G.G.M, et al., 1996, A&A 315, L289
Sakata A., Wada S., Tanabe T., Onaka T., 1984, ApJ 287, L51
Sellgren K., 1984, ApJ 277, 623
Siebenmorgen R., Krügel E., 1992, A&A 259, 614
Siebenmorgen R., Natta A., Krügel E., Prusti T., 1998, A&A in press
Snell R.L., Huang Y.-L., Dickman R.L., Claussen M.J., 1988, ApJ 325, 853
Tran D., Cesarsky D., Sauvage M., 1999, to appear in: Cox P., Demuyt V., Kessler M. (eds.) The Universe as seen by ISO
Tokumaga A., 1984, AJ 89, 172
Verstraete L., Puget J.L., Falgarone E., et al., 1996, A&A 315, L337
Wooden D., 1994, ASP Conference Series 62, 138
Zavagno A., Cox P., Baluteau J.P, 1992, A&A 259, 241
Zavagno A., Ducci V., 1999, to appear in: Cox P., Demuyt V., Kessler M. (eds.) The Universe as seen by ISO